Renewable Energy 139 (2019) 235–241

Contents lists available at ScienceDirect

Renewable Energy

journal homepage: www.elsevier.com/locate/renene

Experimental evaluation of beef drying kinetics in a solar tunnel dryer

Eunice A. Mewa [a, *], Michael W. Okoth [a], Catherine N. Kunyanga [a], Musa N. Rugiri [b]

[a] Department of Food Science, Nutrition and Technology, University of Nairobi, P.O. Box 29053-00625, Nairobi, Kenya
[b] Department of Agricultural Engineering and Technology, Egerton University, P.O. Box 536-20115, Egerton, Kenya

ARTICLE INFO

Article history:
Received 9 August 2018
Received in revised form
11 February 2019
Accepted 13 February 2019
Available online 14 February 2019

Keywords:
Solar tunnel drying
Beef
Drying kinetics
Mathematical modeling
Moisture diffusivity

ABSTRACT

This study focused on the experimental analysis on drying kinetics of beef in a solar tunnel dryer. During the drying process the parameters of drying air were monitored. Experimental drying curves were then determined. The drying data were fitted to five drying models and their constants evaluated by non-linear regression analysis. Validity of the models was assessed using the coefficient of determination (R^2), the reduced chi-square (χ^2), mean relative percent error (P) and root mean square error (E_{RMS}). Effective moisture diffusivity (D_{eff}) of beef was also determined. During the drying period, the ambient temperature, ambient relative humidity, inlet air velocity and solar radiation intensity varied from 21.3 to 38.9 °C, 48–69.5%, 0.02–0.18 m/s and 476.3–1000 W/m^2 respectively. Temperature profile along the tunnel dryer increased with increased solar radiation and decreased continuously at high moisture content of beef. Whereas drying occurred predominantly in the falling rate period for both drying methods, samples dried in the solar drier had a higher drying rate compared to sun dried beef. The most suitable model for representing the drying characteristics of beef was the Page model. The D_{eff} values for solar tunnel dried beef varied from 2.282 10^{-10} to 2.536 $\times$ 10^{-10} m/s^2.

1. Introduction

The most consumed meat product in Sub-Saharan Africa is beef. Its production is highest in South Africa, Kenya, Egypt, Nigeria, Sudan and Morocco respectively [1]. More than 50% of livestock population in Kenya is found in the arid and semi-arid lands under the pastoral production system, which provides the bulk of meat consumed in the country [2]. However, due to the lack of cold storage facilities and climatic conditions in these areas, it is essentially not possible to preserve meat or meat products for any length of time. Meat has a rich nutrient matrix and high water activity, thus highly perishable and can undergo deterioration from time to time. This can result in post-harvest losses which can be as high as 50% of the meat produced, leading to food insecurity and reduced profit margins to value chain actors in Kenya [3].

It is therefore, necessary to adopt technologies which can effectively reduce the post-harvest losses by applying appropriate methods of post-harvest handling, processing and preservation. The most common dryers that are used industrially are the electrically heated hot-air dryers. However, in order to improve the quality of the drying processes of agricultural produce, new drying technologies have come up. Whereas some have improved energy consumption and efficiency like the gas fired hot-air dryers [4] others give higher quality attributes of dried products. These include; superheated steam dryers [5], vacuum dryers [6] and freeze dryers [7].

However, due to their higher energy requirements, these technologies are not applicable and affordable to most farmers in the arid and semi-arid areas. Sun drying is commonly practiced in the developing countries as a method of meat preservation and is still preferred due to the use of solar energy which can serve as a sustainable energy source, is renewable and environment friendly [8]. During open sun drying, the surface of the drying material absorbs solar radiation, which is converted to heat and is conducted to the interior of the bulk. This leads to temperature increase of the drying product and provides energy for transfer of moisture to the air. Natural convection supported by wind energy, then removes the evaporated water [9]. However, the method, exposes the product to contamination by dirt, dust, insects and bacteria [10] causing significant reduction of product quality.

Solar drying can be done as an alternative to open sun drying as it is a promising and attractive application of solar energy systems. This technology is suitable for use in the pastoral areas of Kenya where there is abundant supply of solar energy. Solar dryers are

* Corresponding author.
E-mail address: eunicemewa@yahoo.com (E.A. Mewa).

https://doi.org/10.1016/j.renene.2019.02.067
0960-1481/

classified into two main groups based on the mode of air flow: forced convection and natural convection solar dryers [11]. In a properly designed natural convection dryer, air current can be generated due to density gradient of the air along the dryer [12]. However, the long drying times as a result of the low air flow gives a low drying capacity of the natural convection dryers. Forced convection dryers require a power source for operating an external fan or blower to create air current within the dryer. The forced convection types of dryers include; solar tunnel driers, greenhouse type solar driers, indirect forced convection solar driers and roof integrated solar driers [13,14].

Research on solar tunnel drying of food products in different regions of the tropics and subtropics has mostly covered experimental investigations on dehydration of fruits [15–17], vegetables [18–20] and fish [21,22] and several mathematical models have been applied for simulating the drying kinetics of the products. However, work on experimental investigations on solar tunnel drying kinetics of beef is apparently rarely studied in literature. The present study was therefore undertaken to evaluate the solar tunnel drying kinetics of beef, while comparing the experimental data to data obtained from open sun drying as the control.

2. Materials and methods

2.1. Solar tunnel dryer

Installation of the Hohenheim type solar tunnel dryer was done at Ewaso Ng'iro North Development Authority (ENNDA) premises, Isiolo county, Kenya. The dryer (18 m long, 1.96 m wide and the transparent cover inclined 15° to the horizontal) was placed horizontally on an elevated platform, not shaded by a building or trees and was oriented in a direction that made the capture of the incident solar radiation more efficient (Fig. 1).

Half of the dryer consisted of a flat-plate collector for heating the incoming air and the other half, a tunnel drying chamber, where the product being dried was placed. Plain metal sheets with wooden frames were used at base of the collector and drying chamber in several small sections which were joined together in series. At the bottom of the dryer in between the two metal sheets, an insulation material (glass wool) was used to reduce loss of heat from both the collector and drying chamber. One photovoltaic solar module provided the power to run the two direct-current fans (connected in series), which provided the required airflow within the tunnel dryer. Black paint was used at the collector base to facilitate absorption of solar radiation.

A UV stabilized plastic sheet, was fixed as a sloping roof cover over the collector and the drying chamber to provide greenhouse effect as well as to protect the product from insects and rain. A metal tube was fixed to one end of the plastic sheet, which allowed loading and unloading of the dryer by rolling of the plastic sheet up and down. The operation of the dryer is such that solar radiation gets to the absorber surface by passing through the transparent cover of the collector, providing heat energy which is transferred to the air. From the collector, the heated air then moves to the drying chamber, transfers heat and absorbs moisture from the products thus causing dehydration. Products within the drying chamber are also heated by direct solar radiation passing through the transparent cover.

Fig. 1. Pictorial view of the solar tunnel dryer from the collector end.

2.2. Experimental drying procedure

Experimental drying runs were conducted under the climatic conditions of Isiolo county in the months of August and September 2017. The weather was generally sunny during the drying processes. For all drying experiments, fresh beef of about 5.0 mm thickness were weighed and spread as a single layer on trays (layered with plastic nets) which were loaded into the drying chamber. Each experiment was started at 9:00 a.m. (after completion of loading) and discontinued at 4:00 p.m. The drying section of the tunnel dryer was divided into four equal sub-sections in order to evaluate drying kinetics of beef at different areas of the dryer. Control samples of beef were placed on a raised platform beside the drier and spread out as a single layer, allowing air to pass from beneath the tray. This was done to compare the solar tunnel dryer performance with dehydration in the open sun. At the beginning of drying, moisture loss from the samples was determined by weighing samples from one point of each tray (from each sub-section of the drying chamber) after every 30 min, and during the last stage of the process, after every 1 h, using a digital electronic balance (ESA 600, Salter Brecknell, UK: accuracy ±0.01 g) placed outside the tunnel dryer. The weighing process for each sample was done within 1 min to minimize absorption of moisture from ambient air. At 4:00 p.m., the beef slices were collected and placed in a room at ambient conditions, then loaded again the next morning to continue with the drying process. The drying process occurred simultaneously for both the experimental and control samples under the same weather conditions and this was done in duplicates.

During the drying process, air temperature and relative humidity (both ambient and for the drying air), air velocity at collector inlet and solar radiation intensity were measured. Ambient and drying air relative humidity and temperature sensors were placed outside and within the tunnel dryer respectively and data collected by data logger units connected to the sensors. The sensors were inserted at the inlet of the four sub-sections (A, B, C and D) of the drying compartment from the collector end to the end of the drying chamber of the tunnel dryer respectively. The points of insertion of the probes were labeled (1–5) from the beginning of sub-section A to the end of subsection D respectively. An anemometer (Model Taylor 3132, Taylor Instruments, Toronto, Canada: accuracy ±0.01 m/s) was used to measure drying air velocity after every one hour. A pyranometer, placed on a raised horizontal surface outside the dryer and connected to a data logger unit was used for solar radiation intensity measurement. The temperature, relative humidity and pyranometer data logger units recorded data after every five seconds. The drying process was completed on the second day after a total drying time of 11 h for all the samples. Approximately 20 kg of fresh beef slices were dried to approximately 7.5 kg of dried beef samples. They were then cooled and sealed in plastic bags.

2.3. Analysis of drying data

2.3.1. Experimental drying curves

Calculation of moisture content was done as shown below:

$$M_t = \frac{(W_0 - W) - W_1}{W_1} x100 \quad (1)$$

where M_t is the moisture content (% dwb) at time t, W_0 is initial sample weight (g), W is the amount of evaporated moisture (g), and W_1 is dry matter content of sample (g).

Drying curves were presented in terms of moisture content vs drying time and drying rate vs moisture content graphs. The drying rate (DR) of beef slices was calculated using the following equation:

$$DR = \frac{M_t - M_{t+\Delta t}}{\Delta t} \quad (2)$$

where $M_{t+\Delta t}$ is the moisture content at time 't+Δt' (% dwb) and t is time (min).

2.3.2. Mathematical modeling

The relationship between moisture content (% dwb) as a function of drying time (t) was expressed as:

$$\frac{M_t - M_e}{M_0 - M_e} = f(t) \quad (3)$$

The left hand side of the equation (3) is denoted as moisture ratio (MR) as follows:

$$MR = \frac{M_t - M_e}{M_0 - M_e} \quad (4)$$

where MR is the moisture ratio, M_e is equilibrium moisture content (% dwb), M_t is moisture content at any time (% dwb) and M_0 is the initial moisture content (% dwb).

However, owing to the continuous relative humidity fluctuations of drying air during the process of solar drying, determination of M_e becomes a challenge [19]. The equation can therefore be reduced to

$$MR = \frac{M_t}{M_0} \quad (5)$$

The drying data were analyzed in terms of moisture ratio vs drying time graphs. Fitting of the experimental data obtained was done by application of five semi-theoretical models presented in Table 1 [23–28],.

The drying rate constants and coefficients of drying models were estimated using a non-linear regression procedure using the iterative non-linear least square fitting method of Excel 2008 software. The statistical validity of the models were assessed and compared by using the coefficient of determination (R^2), reduced chi-square (χ^2), root mean square error (E_{RMS}) and mean relative percent error (P). The parameters were calculated as follows: (Equations (11)–(14)).

$$R^2 = 1 - \left(\frac{\sum_{i=1}^{N} (MR_{exp,i} - MR_{pre,i})^2}{\sum_{i=1}^{N} (MR_{exp,i} - MR_{pre,i})^2} \right) \quad (11)$$

$$\chi^2 = \frac{\sum_{i=1}^{N} (MR_{exp,i} - MR_{pre,i})^2}{N - z} \quad (12)$$

$$E_{RMS} = \left(\frac{1}{N} \sum_{i=1}^{N} (MR_{exp,i} - MR_{pre,i})^2 \right)^{\frac{1}{2}} \quad (13)$$

$$P = \frac{100}{N} \sum_{i=1}^{N} \frac{|MR_{exp,i} - MR_{pre,i}|}{MR_{exp,i}} \quad (14)$$

where $MR_{exp,i}$ is the ith experimental moisture ratio, $MR_{pre,i}$ is the predicted dimensionless moisture ratio, $MR_{exp,avg}$ is the average experimental moisture ratio, N is the number of observations and z is the number of constants.

R^2 was used as the primary comparison criteria for determining the goodness of fit of the models to the curves. A higher R^2 value and lower values of χ^2, E_{RMS} and P for the models were considered to have better fits.

2.3.3. Effective moisture diffusivity determination

The rate of internal moisture transfer within the meat during drying was described by an effective diffusivity (D_{eff}). The effective moisture diffusivity of the samples was estimated by using the simplified Fick's second diffusion model as given below:

$$\frac{\partial M}{\partial t} = \nabla \left[D_{eff} (\nabla M) \right] \quad (15)$$

where effective moisture diffusivity (m^2/s) is given by D_{eff} (the term used to represent all moisture transport mechanisms within a sample), t is time (s) and M is the local moisture content (% dwb).

The solution of Fick's second law, with the assumption of moisture migration by diffusion, constant diffusion coefficient and temperature, negligible shrinkage and infinite slab geometry as given by Crank [29], was used

$$MR = \frac{8}{\pi^2} \sum_{N=0}^{\infty} \frac{1}{(2n+1)^2} \exp\left(- \frac{(2n+1)^2 \pi^2 D_{eff} t}{4L^2} \right) \quad (16)$$

where n represents a positive integer and L the slab's half thickness (m).

Only the first term of Equation (17) is normally applied, giving:

$$MR = \frac{8}{\pi^2} \exp\left(- \frac{\pi^2 D_{eff} t}{4L^2} \right) \quad (17)$$

Effective moisture diffusivity was obtained by plotting experimental drying data in terms of ln (MR) versus time (s). After

Table 1
Mathematical models used for the solar drying curves.

Model	Equation	References
Newton	$MR = \exp(-kt)$	[23]
Logarithmic	$MR = a\exp(-kt) + c$	[24]
Page	$MR = exp(-kt^n)$	[25,26]
Handerson and Pabis	$MR = a\exp(-kt)$	[27]
Two-term exponential	$MR = aexp(-kt) + (1-a)exp(-kat)$	[28]

Where t is time (min), k is the drying rate constant (min^{-1}) and a, n and c are drying constants.

determining the slope of the straight line, D_{eff} was calculated using the following equation [30].

$$D_{eff} = \frac{-slope\ 4L^2}{\pi^2} \quad (18)$$

3. Results and discussion

3.1. Parameters of drying air

The ambient temperature and solar radiation intensity during the drying period (August–September 2017) varied from a minimum of 21.3 °C to a maximum of 38.9 °C and from 476.3 to 1000 W/m^2 respectively. The ambient relative humidity ranged from 48 to 69.5% whereas the average air velocity at the collector inlet of the solar tunnel dryer varied from 0.02 to 0.18 m/s. Fig. 2 shows variations of the ambient air temperature and solar radiation intensity for a typical day during solar drying of beef samples in August 2017. The ambient air temperature and solar radiation reached their highest values at around 12:00 noon.

The drying temperature at any time in solar tunnel dryer was greater than the ambient temperature, whereas the relative humidity in the tunnel was lower than the ambient relative humidity. Fig. 3 shows the variations of the ambient temperature and relative humidity at the collector outlet with the time of day during solar drying for a typical day of September 2017. The drying temperature and relative humidity at this point in solar tunnel dryer varied continuously from morning to evening. The temperature and relative humidity of drying air ranged from 36.1 to 60.1 °C and 16.5–28.3% respectively. A close relationship between temperature and humidity was observed where relative humidity was high at low temperatures and vice-versa.

Fig. 4 shows the temperature variations along the length of the drying chamber at different times during a typical day of drying in the solar tunnel dryer.

The temperatures inside the solar tunnel dryer ranged from 46.2 to 64.6, 42 to 64.8, 41.5 to 63.4, 40 to 62.5 and 36.1–60.1 °C from the collector end to the end of the drying chamber respectively. The highest temperature (64.8 °C) was recorded at 14:00 h at the sensor positioned 2.25 m from the collector end of the dryer, while the lowest temperature (36.1 °C) was recorded at 9:00 h at the end of the drying chamber. The temperatures were observed to be highest between 12:00 a.m. and 2:00 p.m. During this period, there was minimum variation in drying temperatures within the drying chamber. This could be attributed to regulation by the air flow rate in the dryer. During the high insolation period, more energy is

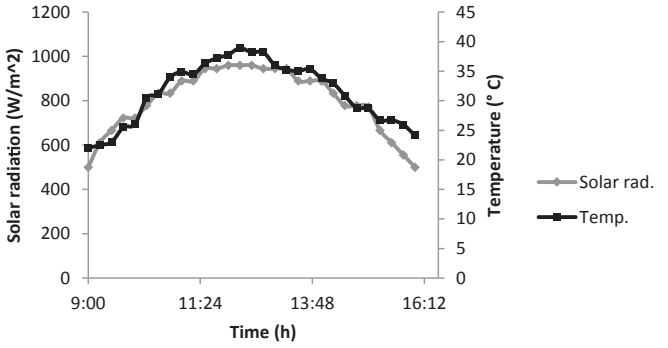

Fig. 2. Variation of the ambient air temperature and solar radiation intensity for a typical day during solar drying of beef samples.

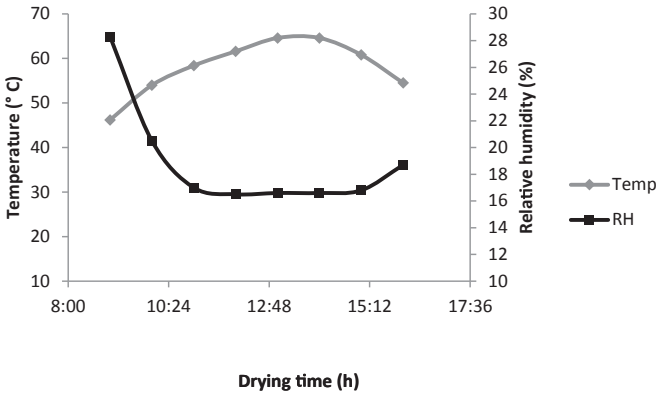

Fig. 3. Variation of the ambient temperature and relative humidity at the collector outlet with time of day during drying in a solar tunnel dryer.

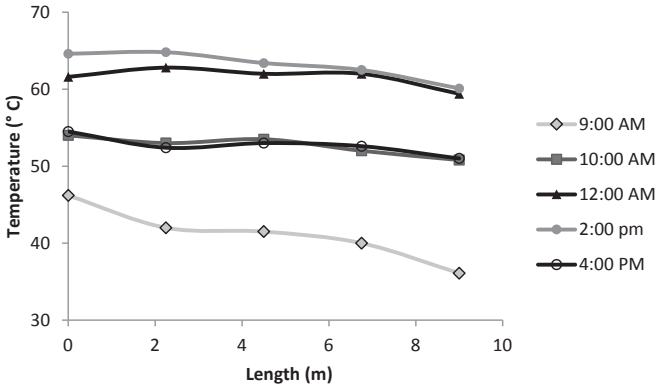

Fig. 4. Variation of temperature with time of day along the length of the drying chamber for a typical day of drying in a solar tunnel dryer.

received by the collector which is intended to increase the drying air temperature. However, this is compensated by the increase of the air flow rate due to more solar energy received by the PV solar module, providing more driving power to the fans [16].

Air temperature decreased along the length of the dryer during the first day of drying and this decrease was more pronounced during the early phase of drying (9:00 a.m., Fig. 4). During this phase, when the moisture content of the product is still high, heated air from the collector section provides the latent heat of vapourization and also mixes with moisture from the material and is continuously cooled as it passes through the dryer section towards the outlet of the tunnel dryer. Similar results were reported by Schirmer et al. [15], and Hossain and Bala [18], who found that temperature profile along the dryer depended not only on the solar radiation but also on the moisture content of bananas and hot chilli being dried in a solar tunnel dryer respectively.

3.2. Experimental drying curves

Fig. 5 shows the moisture content of beef as a function of drying time during open sun drying and solar drying in different sections of the drying chamber. The moisture content decreased considerably with increasing drying time. The moisture content of beef decreased from 309.39% to between 2.32 and 9.56% (dry weight basis/dwb) after 11 h of drying in the different sections of the solar tunnel drier (A-D) while it took the same time to bring down the moisture content in a similar sample to 24.76% (dwb) with traditional sun drying method. This showed that open sun drying

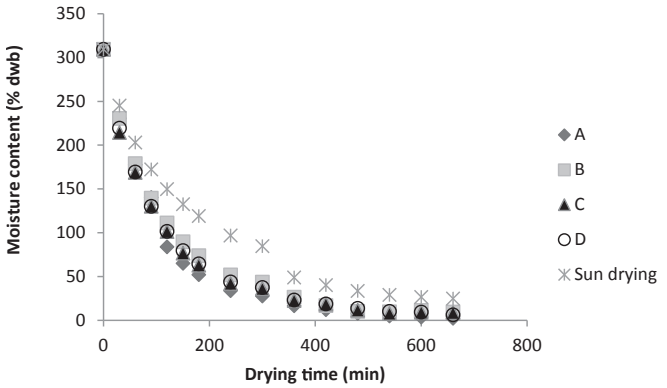

Fig. 5. Moisture content vs drying time graph during beef drying at different sections of the solar tunnel dryer (A–D) compared to open sun drying.

process required a longer time to reduce the moisture content of beef to the same level as samples dried in the solar tunnel dryer. The graphs of solar dried samples showed slightly more variation on the first day of drying between the second to the fifth hour with section A, closest to the collector end of the tunnel dryer having a higher drying rate. This could be attributed to the higher temperatures encountered in this section (Fig. 4).

The beef inside the tunnel dryer lost moisture faster because it received energy from incident solar radiation as well as more energy transported from the collector by forced convection. The control samples on the other hand, received energy from incident solar radiation and less energy transported from surrounding environment by natural convection. Moreover, a significant amount of heat energy was also lost to the environment [18]. This caused the temperature in the dryer to be higher than the ambient temperature and the corresponding relative humidity to be lower than the ambient relative humidity so that the moisture carrying capacity of the air was increased. Generally, the moisture absorption capacity of air is affected by the absolute humidity of the air entering the collector as well as the temperature to which it is subsequently heated.

Fig. 6 shows a graph representing the drying rate versus moisture content during solar tunnel drying (section B) and sun drying of beef. Drying rate of beef in the solar tunnel dryer was higher than for sun dried beef samples.

Drying occurred predominantly in the falling rate period in both the solar tunnel dryer and during open sun drying. During this period, drying rate is controlled predominantly by diffusion of moisture from the interior of food material to its surface and it decreases continuously with decreased moisture content and increased drying time [19]. Beef is considered as a porous medium with the pores acting as channels for water transfer within the meat. The decrease in drying rate with decreased moisture content of beef can be attributed to the diminishing presence of water in its free form as the moisture-food interactions become stronger [31]. These results were in agreement with those of Sacilik et al. [19], for drying tomatoes in a solar tunnel dryer.

3.3. Mathematical modeling

Tables 2 and 3 show the drying coefficients and evaluation criteria used to compare the statistical validity of fits of the five drying models to the experimental data for beef dried in Section D (closest to the outlet of the drying tunnel) compared to open sun drying respectively.

The fitting quality of the models to the experimental data was

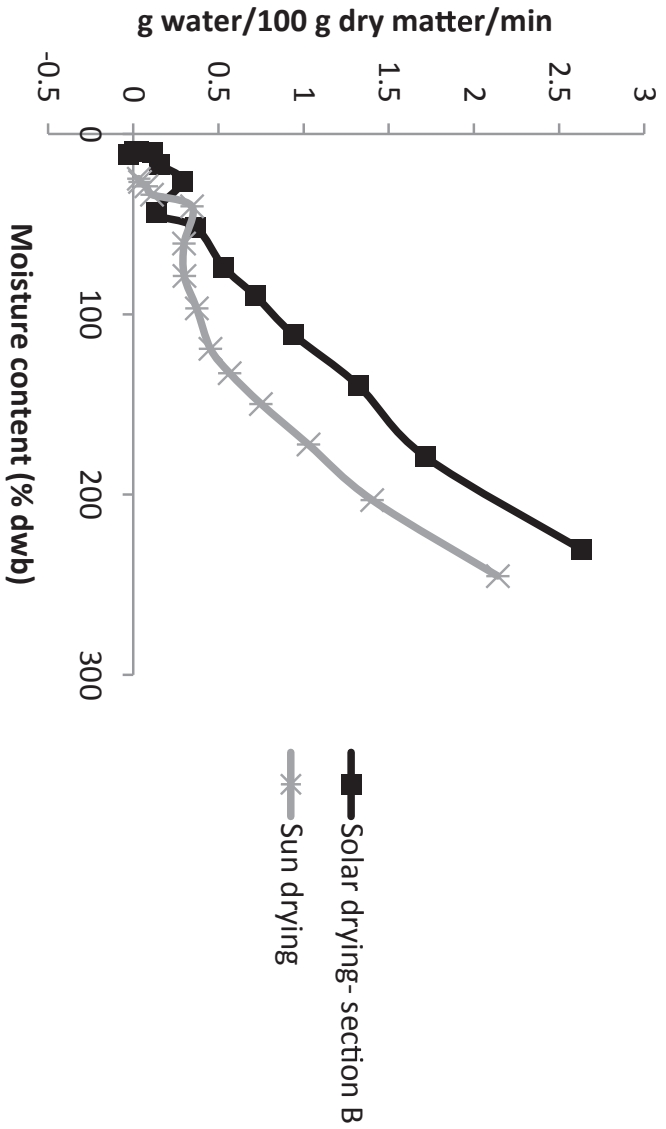

Fig. 6. Drying rate vs moisture content graph during solar and sun drying of beef.

better for solar tunnel drying than for open sun drying, with the values of R^2 greater than 0.99 (Table 2) whereas for sun drying, only the page and two-term exponential models had R^2 values greater than 0.99 (Table 3).

However, for both drying methods, page model gave the highest R^2 values followed by the two-term exponential model. The values for *P* obtained for the Page and logarithmic models for both drying methods were less than 10%, which is in the acceptable range. These models also gave the lowest values of E_{RMS} and χ^2 compared to the other models. Therefore, the Page model was considered the best model in the present study to represent the solar tunnel and sun drying behaviour of beef. As expected, the drying rates represented by k values for all the thin layer drying models (Tables 2 and 3), were higher at the drying chamber of the solar tunnel dryer compared to open sun drying.

Fig. 7 represents the comparison between experimental and predicted values of moisture ratio with drying time using the Page model for sun and solar dried beef samples at different dryer sections. It can be seen from the curves that there was a good agreement between experimental and predicted moisture ratios. This indicates the suitability of the Page model in describing the drying

Table 2
Estimated parameters and comparison criteria of moisture ratio for solar dried beef samples.

Model	Model constants		R^2	E_{RMS}	P	χ^2
Newton	k	0.009056	0.995733	0.030503	32.2638	0.000997
Page	n	0.802121				
	k	0.023376	0.998872	0.00984	8.291977	0.000112
Logarithmic	a	0.87343				
	c	0.032329				
	k	0.008816	0.9948529	0.009348	4.221706	0.000109
Handerson and Pabis	a	0.956391				
	k	0.008578	0.993716	0.027484	29.44735	0.000872
Two-term exponential	a	0.284285				
	k	0.023655	0.998815	0.013127	16.54509	0.000199

Where R^2, E_{RMS}, P and χ^2 are coefficient of determination, root mean square error, mean relative percent error and reduced chi-square respectively.

Table 3
Estimated parameters and comparison criteria of moisture ratio for sun dried beef.

Model	Model constants		R^2	E_{RMS}	P	χ^2
Newton	k	0.00531	0.989623	0.04373	13.20134	0.002049
Page	N	0.782733				
	k	0.016745	0.996547	0.016153	0.874373	0.000301
Logarithmic	a	0.843103				
	c	0.046292				
	k	0.00514	0.9886215	0.018022	0.019305	0.000406
Handerson and Pabis	a	0.925318				
	k	0.004785	0.985747	0.034661	8.915734	0.001386
Two-term exponential	a	0.196418				
	k	0.021334	0.996096	0.020104	4.110848	0.000466

Where R^2, E_{RMS}, P and χ^2 are coefficient of determination, root mean square error, mean relative percent error and reduced chi-square respectively.

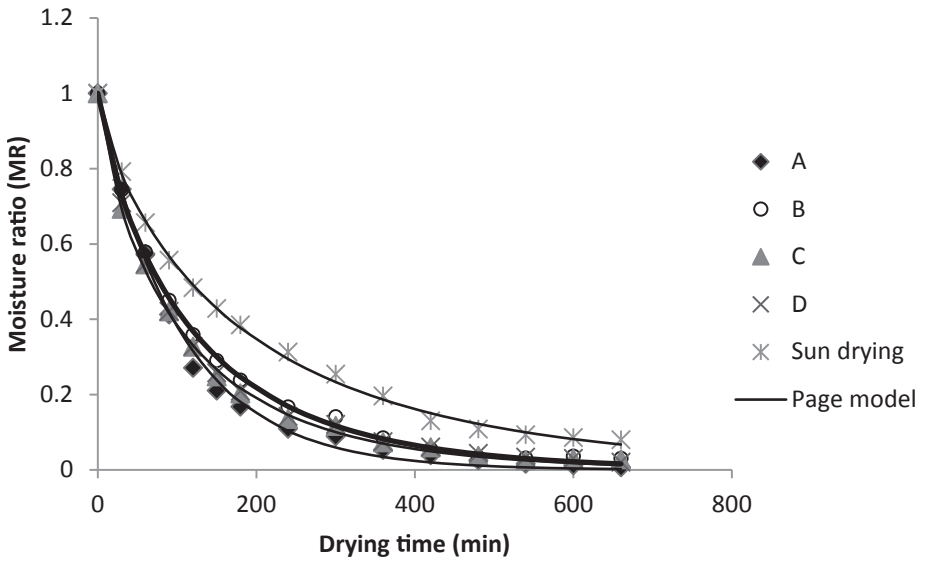

Fig. 7. Variation of predicted and observed moisture ratios against drying time using page model for beef dried at different drier sections (A–D) and in the open sun.

behaviour of beef. The suitability of the page model for describing the solar tunnel drying behaviour of other foods has also been established by Ref. [17].

3.4. Effective moisture diffusivity (D_{eff})

Values for D_{eff} were calculated by using Equation (14) from the slopes of straight lines generated from plots of experimental drying data, ln (MR) vs drying time (Fig. 8).

The effective diffusivity (m^2/s) for solar dried beef was 2.536×10^{-10} at the dryer section closest to the collector outlet (section A) and a constant value of 2.282×10^{-10} for beef dried in the subsequent sections (sections B, C and D). The D_{eff} value for samples dried in the open sun was 1.775×10^{-10}. Section A of the drying chamber in the tunnel dryer generally exhibited on average a higher temperature of drying air during the solar drying process, resulting in higher activity of water molecules in the product [32] and thus a higher D_{eff} value. The values of D_{eff} for beef samples in the solar tunnel dryer were generally higher than for open sun drying. The values of effective diffusivity were within the standard range for food products ($10^{-9} - 10^{-11}$ m^2/s [33]); and could be compared to the reported values of 1.31×10^{-9} to 1.07×10^{-9} m^2/s

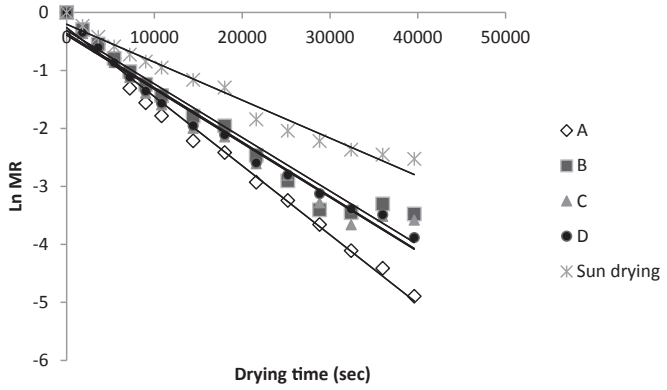

Fig. 8. Linear relationship between logarithmic moisture ratio (ln MR) and drying time at for beef dried at different dryer sections (A–D) and for sun dried beef.

for organic tomato [19] and 1.66×10^{-11} to 1.94×10^{-11} m^2/s for pumpkin [20] during sun and solar tunnel drying of the food products.

4. Conclusions

A solar tunnel dryer (Hohenheim type) can be used for effective drying of beef under the climatic conditions of Isiolo county in Kenya. The moisture content can be reduced to between 2.32 and 9.56% (dwb) in 11 h of drying in the solar tunnel compared 24.76% (dwb) in a similar sample with traditional sun drying method. All drying processes of beef occur in the falling rate period. The Page model adequately describes the solar drying behaviour of beef in a solar tunnel dryer. The Effective moisture diffusivity values for solar tunnel dried beef samples vary from 2.282 to 2.536×10^{-10} m^2/s and is higher than for samples dried in the open sun.

Acknowledgements

The authors gratefully acknowledge the University of Kassel in Germany, for funding the investigation and Ewaso Ng'iro North Development Authority (ENNDA) in Isiolo county, Kenya for their technical support.

References

[1] FAOSTAT, Food and Agriculture Organization of the United Nations, 2016. Statistics Division. [accessed 2017 Jan 12], http://faostat3.fao.org/home/E.
[2] A.K. Kahi, C.B. Wasike, T.O. Rewe, Beef production in the arid and semi-arid lands of Kenya: constraints and prospects for research and development, Outlook Agric. 35 (2006) 217–225.
[3] A.K. Lewa, Evaluation of Animal Health Care Delivery Systems in Selected Areas of Kenya, Phd thesis, University of Nairobi, 2010.
[4] H.S. EL-Mesery, G. Mwithiga, Comparison of a gas fired hot-air dryer with an electrically heated hot-air dryer in terms of drying process, energy consumption and quality of dried onion slices, Afr. J. Agric. Res. 7 (2012) 4440–4452.
[5] A. Speckhahn, G. Srzednicki, D.K. Desai, Drying beef in superheated steam, Dry. Technol. 28 (2010) 1072–1082.
[6] J. Arnau, X. Serra, J. Comaposada, P. Gou, M. Garriga, Technologies to shorten the drying period of dry-cured meat products, Meat Sci. 77 (2007) 81–89.
[7] M.K. Krokida, V.T. Karathanos, Z.B. Maroulis, Effect of freeze-drying conditions on shrinkage and porosity of dehydrated agricultural products, J. Food Eng. 35 (1998) 369–380.
[8] W.T. Xie, Y.J. Dai, R.Z. Wang, K. Sumathy, Concentrated solar energy applications using fresnel lenses: a review, Renew. Sustain. Energy Rev. 15 (2011) 2588–2606.
[9] I.C. Kemp, Fundamentals of energy analysis of dryers, in: E. Tsotsas, A.S. Mujumdar (Eds.), Modern Drying Technology Volume 4: Energy Savings, Wiley-VCH, Weinheim, Germany, 2012, pp. 1–46.
[10] C.L. Hii, C.L. Law, S. Suzannah, Drying kinetics of the individual layer of cocoa beans during heat pump drying, J. Food Eng. 108 (2012) 276–282.
[11] O.V. Ekechukwu, B. Norton, Review of solar-energy drying systems II: an overview of solar drying technology, Energy Convers. Manag. 40 (1999) 615–655.
[12] A. Tesfamichael, A. Assefa, Experimental analysis of potato silces drying characteristics using solar dryer, J. Appl. Sci. 13 (2013) 939–943.
[13] S. Janjai, Personal Communication, Silpakorn University, Nakhon Pathom, Thailand, 2004.
[14] P.H. Oosthuizen, An experimental study of simulated indirect solar rice dryer fitted with a small fan, J. Eng. Int. Develop. 3 (1996) 22–29.
[15] P.S. Schirmer, A. Janjai, R. Esper, W. Samitabhindu, Muhlbauer, Experimental investigation of the performance of the solar tunnel dryer for drying bananas, Renew. Energy 2 (1996) 119–129.
[16] B.K. Bala, M.R.A. Mondol, B.K. Biswas, B.L. Das Choudhury, S. Janjai, Solar drying of pineapple using solar tunnel drier, Renew. Energy 28 (2003) 183–190.
[17] A.K. Elicin, K. Sacilik, An experimental study for solar tunnel drying of apple, Tarim Bilimleri Dergisi 11 (2005) 207–211.
[18] M.A. Hossain, B.K. Bala, Drying of hot chilli using solar tunnel drier, Sol. Energy 81 (2007) 8592.
[19] K. Sacilik, R. Keskin, A. Elicin, Mathematical modeling of solar tunnel drying of thin layer organic tomato, J. Food Eng. 73 (2006) 231–238.
[20] K. Sacilik, Effect of drying methods on thin-layer drying characteristics of hull-less seed pumpkin (Cucurbitapepo L.), J. Food Eng. 79 (2007) 23–30.
[21] B.K. Bala, M.R.A. Mondol, Experimental investigation on solar drying of fish using solar tunnel dryer, Dry. Technol. 19 (2001) 427–436.
[22] G.M. Kituu, D. Shitanda, C.L. Kanali, J.T. Mailutha, C.K. Njoroge, J.K. Wainaina, V.K. Silayo, Thin layer drying model for simulating the drying of Tilapia fish (Oreochromis niloticus) in a solar tunnel dryer, J. Food Eng. 98 (2010) 325–331.
[23] A. Fudholi, M.Y. Othman, M.H. Ruslan, M. Yahya, A. Zaharim, K. Sopian, The Effects of drying air temperature and humidity on drying kinetics of seaweed, Recent Res. Geogr. Geol. Energy Environ. Biomed. 19 (2011) 129–133.
[24] P.K. Chandra, R.P. Singh, Applied Numerical Methods for Food and Agricultural Engineers, CRC Press, Boca Raton, 1995, pp. 163–167FL.
[25] I. Doymaz, Drying kinetics of white mulberry, J. Food Eng. 61 (2004) 341–346.
[26] G.E. Page, Factors Influencing the Maximum Rates of Air-Drying Shelled Corn in Thin Layers, M.S. thesis, Department of Mechanical Engineering, Purdue University, Purdue, USA, 1949.
[27] S.M. Henderson, S. Pabis, Grain Drying Theory II. Temperature effects on drying coefficients, J. Agric. Eng. Res. 6 (1961) 169–174.
[28] Y.I. Sharaf-Eldeen, J.L. Blaisdell, M.Y. Hamdy, A model for ear corn drying, Trans. ASAE 23 (1980) 1261–1271.
[29] J. Crank, The Mathematics of Diffusion, 2d Ed., Clarendon Press, 1975.
[30] E.K. Akpinar, Y. Bicer, Modelling of the drying of eggplants in thin-layers, Int. J. Food Sci. Technol. 40 (2005) 273–281.
[31] U.S. Shivhare, S. Arora, J. Ahmed, G.S.V. Raghavan, Moisture adsorption isotherms for mushroom, LWT Food Sci. Technol. 37 (2004) 133–137.
[32] J. Shi, Z. Pan, T.H. Mc Hugh, D. Wood, E. Hirschberg, D. Olson, Drying and quality characteristics of fresh and sugar-infused blueberries dried with infrared radiation heating, LWT Food Sci. Technol. 41 (2008) 1962–1972.
[33] N.P. Zogzas, Z.B. Maroulis, D. Marinos-Kouris, Moisture diffusivity data compilation in foodstuffs, Dry. Technol. 14 (1996) 2225–2253.